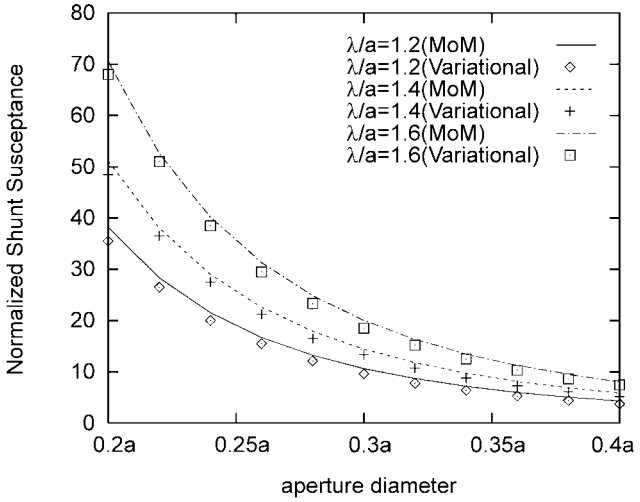


Fig. 4. Normalized susceptance of the centered circular aperture in the cross-sectional plane of a rectangular waveguide ($\lambda$: wavelength).

In comparison, the Ewald sum-based calculations presented in Fig. 2 show very rapid convergence. The average error decreases exponentially as the number of calculated terms increases. In Fig. 2, superscripts $A$ and $F$ desiginates the magnetic- and electric-vector potential functions, respectively. The results shown in this figure have been obtained through averaging Green's function calculations over 625 different source–observation point pairs (25 source points $\times$ 25 observation points) evenly distributed on the same cross-sectional plane of the waveguide ($z = z'$). On average, 18.73 and 22.01 terms were needed to obtain $10^{-4}$ and $10^{-5}$ convergence, respectively. Therefore, the proposed method can achieve sufficient accuracy for most numerical applications with only about 20 term calculations.

The next result concerns the optimum choice of the Ewald sum parameter $E$. In Fig. 3, relative calculation times are given as a function of the parameter $E$. For the small and large values of $E$, the total calculation time increases due to the slow convergence of the spatial and spectral series, respectively. The overall average calculation time is minimized for the $E$ values in the range of $0.6\pi/\sqrt{ab} - 0.9\pi/\sqrt{ab}$ under the proposed calculation schemes.

Finally, Fig. 4 shows the application of the proposed method to the scattering analysis of a centered circular aperture in the cross-sectional plane of the rectangular waveguide [8]. The MoM analysis employed the Galerkin's method with triangular-rooftop basis functions. The aperture has been discretized with 90 triangular elements and 145 basis functions. It took about 30 s to obtain one point data on a Sun UltraSpark1 workstation. The calculated results agree well with those by the variational method [8] within the error bound of the variational formula.

## REFERENCES

[1] B. C. Ahn, "Moment method analysis of a narrow wall inclined slot on a rectangular waveguide," Ph.D. dissertation, Dept. Elect. Eng., Univ. Mississippi, Oxford, 1992.

[2] J. Xu, "Fast convergent dyadic Green's function in a rectangular waveguide," *Int. J. Infrared Millim. Waves*, vol. 30, no. 3, pp. 409–418, May. 1993.

[3] R. E. Jorgenson and R. Mittra, "Efficient calculation of the free-space periodic Green's function," *IEEE Trans. Antennas Propagat.*, vol. 38, pp. 633–642, May 1990.

[4] P. P. Ewald, "Die berechnung optischer und elektrostatischen gitterpotentiale," *Ann. Phys.*, vol. 64, pp. 253–268, 1921.

[5] K. E. Jordan, G. R. Richter, and P. Sheng, "An efficient numerical evaluation of the Green's function for the Helmholtz operator on periodic structures," *J. Comput. Phys.*, vol. 63, no. 16, pp. 222–235, 1986.

[6] M.-J. Park, J. Park, and S. Nam, "Efficient calculation of the Green's function for the rectangular cavity," *IEEE Microwave Guided Wave Lett.*, vol. 8, pp. 124–126, Mar. 1998.

[7] M. Abramowitz and I. Stegun, Eds., *Handbook of Mathematical Functions*. New York: Dover, 1970.

[8] N. Marcuvitz, *Waveguide Handbook*. New York: McGraw-Hill, 1951.

# FDTD Improvement by Dielectric Subgrid Resolution

Gaetano Marrocco, Marco Sabbadini, and Fernando Bardati

***Abstract*— Material inhomogeneities are taken into account in the standard finite–difference time-domain method by staircase modeling of medium boundaries. Resolution is, therefore, limited by Yee's cell sizes. In this paper, a new scheme is proposed, which improves material resolution without increasing the demand of computer resources.**

***Index Terms*—Dielectric inhomogeneity, FDTD method, subgridding.**

## I. INTRODUCTION

The finite-difference time-domain (FDTD) method [1] is well suited to compute electromagnetic-field components, which are tangential to the interface among different dielectric media. Dielectric discontinuities are modeled by plane surfaces through mesh nodal points while each elementary cell is homogeneously filled. To analyze complicated structures, such as irregularly shaped and inhomogeneous microwave devices, it is necessary to use a fine cell size and large computer resources. Moreover, the modeling of curvilinear boundaries [see Fig. 1(a)] requires staircase approximation in order to accommodate the structure to the computational grid. In such a case, the accuracy is related to grid-size refinement, i.e., to computer resources. Halving the cell size improves boundary accommodation [see Fig. 1(b)]. More economical in terms of computational burden, an inhomogeneous cell can be treated as it was homogeneously filled by a medium with parameters $\varepsilon$, $\sigma$, $\mu$, which are obtained by volume averaging of the different media inside the cell. However, this method does not give very accurate results. Alternative formulations have been proposed, which model boundaries by local modification of Maxwell's equations [2]–[4], local grid modification [5], or globally irregular gridding [6], [7]. These methods differ substantially in the modeling of dielectric interfaces and generally require complex algorithms and preprocessing. A different method by Gwarek [8], [9] is based on separate modeling of several kinds of dielectric discontinuities, which may occur when a standard FDTD cell is intersected by a dielectric interface [see Fig. 1(c)]. In this method, a couple of effective parameters is associated to each intersection,

Manuscript received March 10, 1997; revised August 12, 1998.

G. Marrocco and F. Bardati are with DISP, University of Rome "Tor Vergata," 00133 Rome, Italy.

M. Sabbadini is with ESA-ESTEC, AG 2200 Noordwijk, The Netherlands.

Publisher Item Identifier S 0018-9480(98)09063-2.

0018–9480/98$10.00 © 1998 IEEE

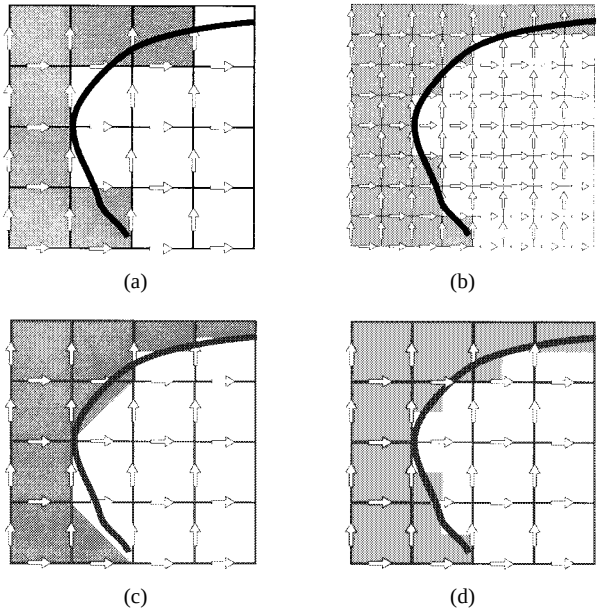


Fig. 1. Approximation of a general boundary between two dielectric media. (a) Staircasing with homogeneously filled cells. (b) Halved homogeneously filled cells. (c) Local discontinuity modeling. (d) Uniform sub-cell partitions, as in DSR.

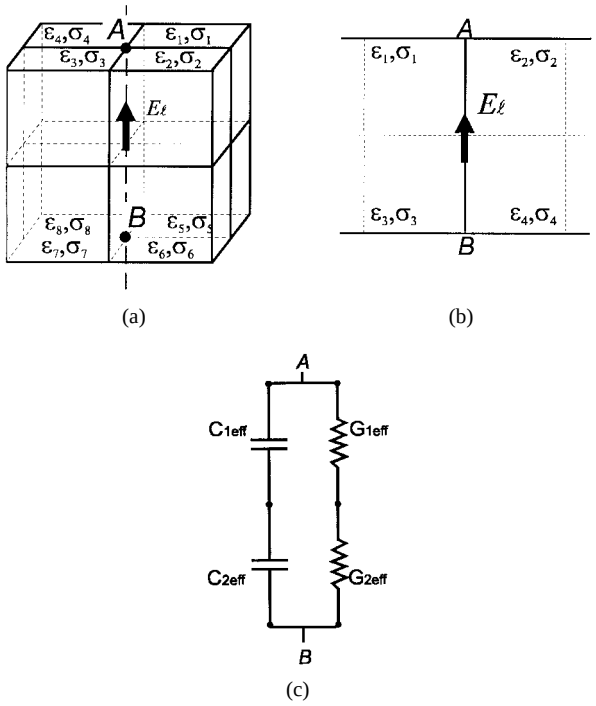


Fig. 2. Wedge discontinuities for three-dimensional (3-D) and 2-D grids and equivalent lumped circuit.

accounting for the dielectric inhomogeneity. The method has been proven to be successful and accurate for the analysis of microwave devices. Nevertheless, it requires preprocessing operations intended to classify the intersections between cells and boundaries and to fill a database of effective parameters.

In this paper, as in Gwarek's method, dielectric discontinuities are taken into account by the use of effective parameters, but the dielectric structure is modeled on a systematic basis more than by the use of local classification of boundary–cell intersections. A dielectric subgrid resolution (DSR) is achieved if each cell is allowed to be filled by different materials in such a way that each FDTD cell is regularly partitioned into eight homogeneously filled sub-cells, which reduce to four sub-cells in a two-dimensional (2-D) problem. Dielectric boundaries, therefore, are allowed to pass through a cell, as in the Gwarek's method, but only conforming to this partitioning scheme [see Fig. 1(d)].

## II. Generalized Constitutive Parameters

In the standard FDTD formulation, the elementary Yee cell (electric-field components along a cube edges) is filled by a homogeneous medium. Dielectric boundaries can be only located between adjacent cells, therefore, they are tangential to the electric-field components. This kind of dielectric discontinuity is referred to as *tangential discontinuity*. Equivalent constitutive parameters have been derived [10], [11] by enforcing the tangential electric- and magnetic-field components in the integral formulation of the Ampere's law to be continuous across the boundary. Such formulation is first-order accurate in cell size and leads to the definition of an effective permittivity and conductivity. These parameters are obtained by averaging the parameters of the neighboring cells with respect to the discontinuity, e.g., the effective permittivity for $E_z(i,j,k)$ is

$$\varepsilon_{\rm eff}(i,j,k) = \tfrac{1}{4}[\varepsilon(i,j,k)+\varepsilon(i-1,j,k)+\varepsilon(i,j-1,k) +\varepsilon(i-1,j-1,k)]. \quad (1)$$

A similar equation holds for $\sigma_{\rm eff}(i,j,k)$. Equation (1) reduces to the standard one in homogeneous regions where the FDTD formulation preserves second-order accuracy. When a cell is allowed to be filled by up to eight different dielectrics, an electric-field component can be perpendicular to a dielectric boundary. In such a case, hereafter referred to as *normal discontinuity*, effective parameters can be derived by enforcing the continuity across the interface of the normal component of electric flux density $\boldsymbol{D}$ and conduction current $\boldsymbol{J}$ in the Newmann–Lenz's law, as in [9] and [12], e.g., the normal discontinuity between two media having parameters $\varepsilon_1$, $\sigma_1$, and $\varepsilon_2$, $\sigma_2$ is accounted for by the following effective parameters:

$$\varepsilon_{\rm eff} = 2\frac{\varepsilon_1\varepsilon_2}{\varepsilon_1+\varepsilon_2} \quad \sigma_{\rm eff} = 2\frac{\sigma_1\sigma_2}{\sigma_1+\sigma_2}. \quad (2)$$

In a general case, an electric-field component at the common point of eight sub-cells (four cells for a 2-D grid) will belong to a dielectric edge (*wedge discontinuity*), resulting at the same time, tangential and normal to dielectric boundaries (see Fig. 2). The effective parameters for this geometry can be derived by using lumped-circuit models. It is known [13] that the FDTD equation which updates an electric component, e.g., $E_z$, is the voltage-balance equation for an electric bipole if the following correspondences hold:

$$\begin{aligned} E_z \leftrightarrow V &= E_z\Delta z \\ \varepsilon \leftrightarrow C &= \varepsilon\frac{\Delta x\Delta y}{\Delta z} \\ \sigma \leftrightarrow G &= \sigma\frac{\Delta x\Delta y}{\Delta z} \end{aligned} \quad (3)$$

where $V$ is voltage, $C$ is capacitance, and $G$ is conductance. $\Delta x$, $\Delta y$, and $\Delta z$ are lengths of the cell sides, $\varepsilon$ and $\sigma$ are parameters of the medium filling the cell. The equivalent capacitance of a tangential (normal) discontinuity is the parallel (series) connection of the corresponding capacitances, each one being evaluated by means of (3).

The equivalent parameters for a wedge discontinuity of $E_z$, which exists in the case of subgrid resolution and eight different media having a common point, can be derived as follows: $C_{1\rm eff}$ and $C_{2\rm eff}$ are equivalent capacitances to account for $E_z$ being tangential to media

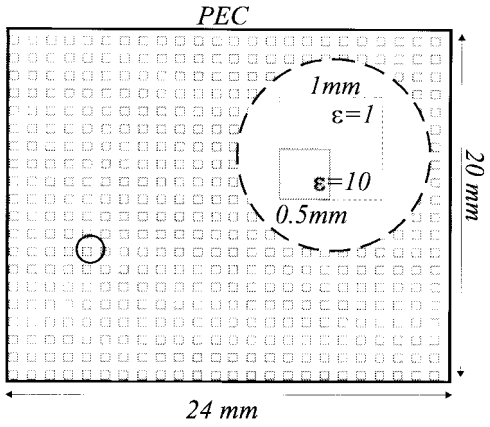


Fig. 3. Periodically loaded cavity as a test case for DSR.

$\varepsilon_1$, $\varepsilon_2$, $\varepsilon_3$, $\varepsilon_4$, and $\varepsilon_5$, $\varepsilon_6$, $\varepsilon_7$, $\varepsilon_8$, respectively. They are computed by (1) and (3) as the parallel of the corresponding capacitances. Next, the normal discontinuity is taken into account by the series of $C_{1\text{eff}}$ and $C_{2\text{eff}}$, as in (2). Similar considerations hold for conductances. The equivalent circuit for a wedge discontinuity is the parallel connection of the found equivalent capacitance and conductance, as in Fig. 2. The constitutive parameters for $E_z$, which account for a wedge discontinuity, are given by

$$\varepsilon_{\text{eff}} = 2\frac{\varepsilon_{\text{eff}}^{(1)}\varepsilon_{\text{eff}}^{(2)}}{\varepsilon_{\text{eff}}^{(1)} + \varepsilon_{\text{eff}}^{(2)}} \quad \sigma_{\text{eff}} = 2\frac{\sigma_{\text{eff}}^{(1)}\sigma_{\text{eff}}^{(2)}}{\sigma_{\text{eff}}^{(1)} + \sigma_{\text{eff}}^{(2)}} \tag{4}$$

where the parameters $\{\varepsilon_{\text{eff}}^{(p)}, \sigma_{\text{eff}}^{(p)}\}_{p=1,2}$ can be obtained from the tangential discontinuity problems according to (1). Finally,

$$\varepsilon_{\text{eff}} = \frac{(\varepsilon_1+\varepsilon_2+\varepsilon_3+\varepsilon_4)(\varepsilon_5+\varepsilon_6+\varepsilon_7+\varepsilon_8)}{2(\varepsilon_1+\varepsilon_2+\varepsilon_3+\varepsilon_4+\varepsilon_5+\varepsilon_6+\varepsilon_7+\varepsilon_8)}. \tag{5}$$

Similar considerations yield the effective permittivity for a 2-D grid [see Fig. 2(b)] as

$$\varepsilon_{\text{eff}} = \frac{(\varepsilon_1+\varepsilon_2)(\varepsilon_3+\varepsilon_4)}{\varepsilon_1+\varepsilon_2+\varepsilon_3+\varepsilon_4}. \tag{6}$$

The above definitions of effective parameters for the computation of $E_z$ include dielectric homogeneity as well as tangential and normal discontinuities as particular cases. The effective parameters for $E_x$ and $E_y$ can be obtained in a similar way. Note that a cell is characterized by three couples of effective parameters, one for each field component. Therefore, a cell partitioned according to DSR appears as it was filled by an equivalent anisotropic medium.

The proposed algorithm allows the modeling of dielectric features smaller than a Yee's cell without a real increase of computer resources. In fact, let $N = I \times J \times K$ be the size of an FDTD computation for a given space step $\Delta$. Computation time and memory storage are directly related to $N$. Instead, the structure is sampled at $\Delta/2$ to apply DSR and, therefore, it is modeled by $8N$ voxels.

## III. Numerical Results and Discussions

Test cases were performed to investigate the capability of the DSR scheme to model wedge discontinuities, and more in general curved dielectric boundaries. For the sake of simplicity, test cases were performed on a 2-D grid.

The first test was the computation of the lowest resonant frequencies of a rectangular cavity (24 mm × 20 mm). The medium inside the cavity exhibits periodicity like a photonic bandgap (PBG) material (see Fig. 3). Resonance frequencies are computed by Gaussian pulse excitation with a 16-GHz band. The reference solution is obtained by a standard FDTD computation with a 0.5-mm grid, which exactly conforms the dielectric structure in the sense that each Yee cell is dielectrically homogeneous. The computation domain is 44 × 40 cells. Results to be validated are obtained using the DSR algorithm with a 1-mm grid. Since the dielectric boundaries pass through the cells, corresponding wedge discontinuities are originated. The resulting grid is 22 × 20, i.e., a quarter of the reference problem. By applying (6), it follows that the medium behaves as a homogeneous one with 1.69 effective permittivity. Note that the volumetrically averaged permittivity is 3.25. Resonant frequencies are reported in Table I for the different models. The results show that the standard FDTD, with coarse grid and averaged permittivity, gives completely wrong results, while at the same computational cost, the DSR scheme is quite sensitive to the subgrid variation of the dielectric filling the resonator.

TABLE I
Resonant Frequencies [Gigahertz] for the Cavity of Fig. 3

| n | FDTD (Δ=0.5mm) | FDTD -averaged (Δ=1mm) | FDTD -DSR (Δ=1mm) |
|---|---|---|---|
| 1 | 7.027 | 4.912 | 6.854 |
| 2 | 10.450 | 7.179 | 9.930 |
| 3 | 14.054 | 9.572 | 13.223 |
| 4 | 15.856 | 10.957 | 15.202 |

As a second test, the near-field scattering from an infinite layered dielectric circular cylinder was computed. The cylinder, having the axis along $z$, is illuminated by a TM monochromatic $x$-directed plane wave. The scatterer was first modeled on a fine mesh with cell $\Delta = 0.0212$ (100 × 100 cells) by means of: 1) standard FDTD; then on a coarser mesh with cell $2\Delta$ (50 × 50 cells) by means of 2) standard FDTD; and 3) FDTD with dielectric subgrid resolution. Accordingly, the outer layer is thick six cells [see 1)] and three cells [see 2) and 3)]. Electric-field amplitudes for the three cases are compared with the analytical solution [14] along a concentric circle of radius $R_3$ (see Fig. 4). This test line is close to the cylinder in such a way to appreciate the local effect of the curved boundary staircasing on the scattered field, which is otherwise attenuated in the far-field region. In this case of TM scattering, normal and wedge discontinuities must be considered for DSR modeling. In TE scattering, only tangential discontinuities are originated, which are automatically accounted for by FDTD. It can be observed that the scattered field is successfully predicted by both the FDTD on a finer mesh and by the FDTD on a coarser mesh with DSR. On the contrary, the standard FDTD on the coarser mesh fails especially in the computation of the peaks of the scattered field. Note that the root-mean-square (rms) error (with respect to the analytical solution) of solutions 1) and 2) are comparable (6%) while it is doubled (12%) for 3).

## IV. Conclusions

The FDTD algorithm has been modified to achieve a better resolution of dielectric interfaces inside the computational domain. In particular, the staircase step is halved along each direction in DSR without affecting Yee's cell size, i.e., the demand of computer resources. To this purpose, a compact and simple definition of the effective constitutive parameters, including the effect of wedge discontinuities, has been presented. The new formulation allows FDTD dielectric resolution to be extended to one-eighth of the elementary cell volume without a local modification of Maxwell's equations.

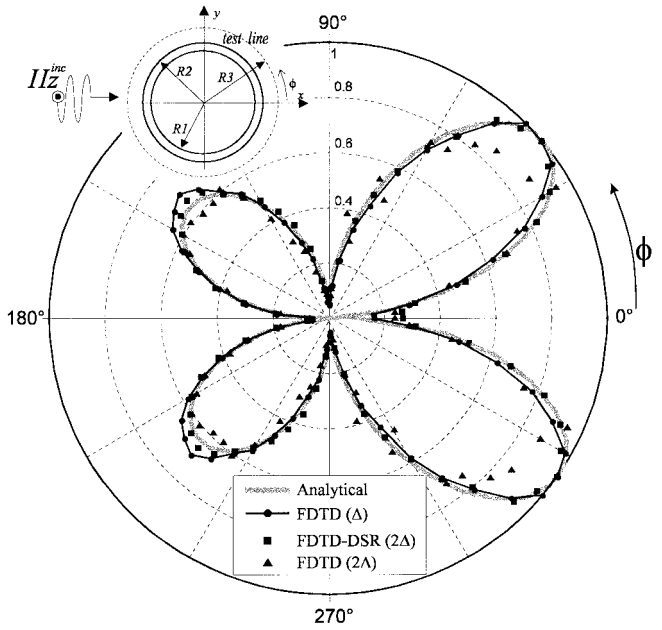


Fig. 4. $|Ex|$ versus angle $\phi$ for TM scattering by a circular layered dielectric cylinder. Inner layer: $\varepsilon_1 = 25$, $\sigma_1 = 1$, $R_1 = 0.17\lambda$. Outer layer: $\varepsilon_2 = 5$, $\sigma_2 = 0.3$, $R_2 = 0.21\lambda$.

Numerical tests were performed to show the accuracy of the new scheme. In particular, it has been shown that the DSR algorithm is well suited for the solution of scattering problems involving curved dielectric boundaries. Results by DSR are as accurate as those obtained by the standard FDTD on a doubly dense grid along each direction. It is possible to achieve a saving of computer resources by a factor of eight (four in 2-D problems). A database of effective parameters is unnecessary since DSR allows a unique formulation of effective parameters to hold for any type of dielectric discontinuity originated by sub-cell partition. The coefficients of the FDTD equations are quite compact and easy to be embedded into existing FDTD codes. The proposed degree of subgrid partitioning is reasonable since a field component of the Yee's scheme is defined for each resulting sub-cell. A further subgridding is possible, but it seems useless because field–component interpolation is required to enforce FDTD equations.

## REFERENCES

[1] K. S. Yee, "Numerical solution of initial boundary value problems involving Maxwell's equations in isotropic media," *IEEE Trans. Antennas Propagat.*, vol. AP-14, pp. 302–307, May 1966.

[2] T. Jurgens, A. Taflove, K. Umashankar, and T. Moore, "Finite difference time domain modeling of curved surfaces," *IEEE Trans. Antennas Propagat.*, vol. 40, pp. 357–365, Apr. 1992.

[3] D. B. Shorthouse and C. J. Railton, "The incorporation of static field solutions into the finite difference time domain algorithm," *IEEE Trans. Microwave Theory Tech.*, vol. 40, pp. 986–994, May 1992.

[4] J. G. Maloney and G. Smith, "The efficient modeling of thin material sheets in the finite difference time domain (FDTD) method," *IEEE Trans. Antennas Propagat.*, vol. 40, pp. 323–330, Mar. 1992

[5] D. T. Prescot and N. V. Shuley, "A method for incorporating different sized-cells into the finite-difference time-domain analysis technique," *IEEE Microwave Guided Wave Lett.*, vol. 2, pp. 434–436, Nov. 1992.

[6] P. Harms, J. F. Lee, and R. Mittra, "A study of nonorthogonal FDTD method versus the conventional FDTD technique for computing resonant frequencies of cylindrical cavities," *IEEE Trans. Microwave Theory Tech.*, vol. 40, pp. 741–745, Apr. 1992.

[7] D. Lynch and K. Paulsen, "Time-domain integration of the Maxwell equations on finite elements," *IEEE Trans. Antennas Propagat.*, vol. 38, pp. 1933–1942, Dec. 1990.

[8] W. K. Gwarek, "Analysis of an arbitrarily-shaped planar circuit—A time-domain approach," *IEEE Trans. Microwave Theory Tech.*, vol. MTT-33, pp. 1067–1072, Oct. 1985.

[9] M. Cheluch-Marcysiak and W. K. Gwarek, "Higher-order modeling of media interfaces for enhanced FDTD analysis of microwave circuits," in *Proc. European Microwave Conf.*, Cannes, France, 1994.

[10] A. Reinex and B. Jecko, "Analysis of microstrip patch antennas using finite difference time domain method," *IEEE Trans. Antennas Propagat.*, vol. 37, pp. 1361–1369, Nov. 1989.

[11] K. S. Kunz and R. Luebbers, *The finite Difference Time Domain Method.* Boca Raton, FL: CRC Press, 1993.

[12] G. Marrocco, "FDTD modeling of dielectric discontinuities," Elect. Eng. Dept., Univ. L'Aquila, L'Aquila, Italy, ESA Rep., Contract 11476-95-NL-NB, 1995.

[13] A. Taflove, *Computational Electrodynamics: The Finite Difference Time Domain Method*. Norwood, MA: Artech House, 1995.

[14] J. R. Wait, *Introduction to Antennas and Propagation*. Stevenage, U.K.: Peregrinus, 1994, pp. 162–165.